High Accumulation of Fluorine-18-Fluorodeoxyglucose in Turpentine-Induced Inflammatory Tissue

Susumu Yamada, Kazuo Kubota, Roko Kubota, Tatsuo Ido and Nobuaki Tamahashi

Department of Nuclear Medicine and Radiology, Institute of Development, Aging and Cancer and Cyclotron and Radioisotope Center, Tohoku University; and Clusterecore Institute of Biology, Sendai, Japan

Fluorine-18-2-deoxy-2-fluoro-D-glucose ([^{18}F]FDG) uptake and distribution in an experimentally induced inflammatory tissue were investigated. **Methods:** Rats were subcutaneously inoculated with turpentine oil to induce inflammation and used for tissue distribution studies and autoradiography. **Results:** Time course study of [^{18}F]FDG tissue distribution showed that the uptake in inflammatory tissue increased gradually until 60 min and then decreased. A longitudinal study of [^{18}F]FDG tissue distribution showed that the uptake increased progressively to a peak 4 days after inoculation and then decreased. On the fourth day postinoculation, a section of inflammatory tissue showed characteristic changes of chronic inflammation. Macro- and micro-autoradiography showed a high density of silver grains in the abscess wall consisting of an inflammatory cell layer and granulation tissue. Grain counting on micro-autoradiography of the abscess wall showed that the highest grain density was found in the marginal zone of young fibroblasts, endothelial cells of vessels and phagocytes of neutrophils and macrophages, followed by that in the neutrophil layer and granulation tissue. **Conclusion:** Our results indicate that [^{18}F]FDG PET may be useful in detecting and monitoring chronic inflammatory processes.

Key Words: fluorine-18-fluorodeoxyglucose; inflammation; tissue distribution study; autoradiography

J Nucl Med 1995; 36:1301–1306

Fluorine-18-2-deoxy-2-fluoro-D-glucose ([^{18}F]FDG) as a parameter of glucose metabolism has been widely used for assessing various diseases and treatment evaluation in PET (*1–7*), and is a useful tracer for tumor detection due to its increased glucose utilization. On the other hand, turpentine-induced inflammatory tissue is imaged with a ^{67}Ga-citrate scintigram clearly but not with [^{18}F]FDG (*8*). The results of these studies suggest that the use of [^{18}F]FDG uptake is suitable in differentiating between tumor and inflammation. However, clinical PET studies demonstrating a high [^{18}F]FDG uptake by abscess (*9–12*) have revived the interest in the use of [^{18}F]-FDG in imaging inflammation.

Increased uptake of glucose in inflammatory tissue has been demonstrated in several injury models. Wilmore et al. studied burn patients 8–22 days after injury and reported increased glucose uptake in extremities that had sustained extensive burns (*13*). In addition, Nelson et al. demonstrated increased ^{14}C-glucose uptake 3 days after injury in injured hindlimbs of rats subjected to unilateral hindlimb scalding (*14*). Tischler et al. showed increased uptake of 2-[^{3}H]-deoxyglucose (^{3}H-DG) 2 days after injury in the injured soleus muscle of rats subjected to blunt trauma (*15*). Finally, Daley et al. showed increased ^{14}C-glucose uptake 3 and 5 days after injury in the lambda-carrageenan hindlimb wound model in rats (*16*). These results of increased uptake of glucose, ^{14}C-glucose and ^{3}H-deoxyglucose can account for the high [^{18}F]FDG uptake by human abscess (*9–12*). Although ^{3}H- or ^{14}C-deoxyglucose and [^{18}F]FDG are analogs of deoxyglucose, they are chemically different substances. In fact, there is also a difference in uptake between ^{14}C-deoxyglucose and [^{18}F]FDG in the brain of experimental animals (*17–19*). Therefore, a direct link for increased [^{18}F]FDG uptake and examination of [^{18}F]FDG distribution in inflammatory tissue with the same tracer used in clinical PET is required to understand these processes. The purpose of this study was to investigate [^{18}F]FDG uptake and distribution in turpentine-induced inflammatory tissue.

MATERIALS AND METHODS

Animals and Inflammation Model

The protocol was fully approved by the Laboratory Animal Care Committee of Tohoku University. Male Donryu rats weighing 80–100 g were used in all experiments. They were housed under constant environmental conditions with 12–12 hr light-dark cycles. Food and water were provided ad libitum. To induce inflammation, animals were inoculated with 0.2 ml of turpentine oil subcutaneously in the left groin region.

Received Jul. 15, 1994; revision accepted Jan. 12, 1995.

For correspondence or reprints contact: Susumu Yamada, MD, Department of Nuclear Medicine and Radiology, Institute of Development, Aging and Cancer, Tohoku University, 4-1 Seiryo-cho, Aoba-ku, Sendai 980, Japan.

Time-Course Study of Fluorine-18-FDG Tissue Distribution

Animals were selected 4 days after inoculation since maximum [^{18}F]FDG uptake was observed on the same day during the longitudinal study (see below). Rats were injected with 740 kBq (20 μCi) of [^{18}F]FDG through the tail vein. They were killed 1, 5, 10, 20, 40, 60 and 120 min postinjection (n = 5, each). The inflammatory tissue sample, including inoculated turpentine-oil, was excised and trimmed of the neighboring subcutaneous tissue. The muscle of the right thigh was excised and blood was collected from the heart. Each sample was weighed and the ^{18}F radioactivity was counted with a well-type NaI(Tl) autogamma counter and corrected for decay. Data were expressed as the differential uptake ratio (DUR) (*20*).

$$\text{DUR} = \frac{\text{tissue counts(cpm)/tissue weight(g)}}{\text{injected RI counts(cpm)/animal body weight(g)}}.$$

Longitudinal Study of Fluorine-18-FDG Tissue Distribution

A dose of 740 kBq (20 μCi) [^{18}F]FDG was injected intravenously through the tail vein at 1, 2, 4, 7 and 14 days postinoculation (n = 5, each). Another five rats without inoculation were used as controls (0 day after inoculation). Animals were killed 1 hr after injection and tissue samples were excised and weighed, followed by counting ^{18}F radioactivity. Data were also expressed as DUR.

A portion of each inflammatory tissue sample was fixed in a conventional 10% neutral-buffered formalin, dehydrated in graded alcohol and finally embedded in paraffin. Thin sections were stained with hematoxylin and eosin (H&E) for histological examination.

Macro-Autoradiography and Micro-Autoradiography

A dose of 74 MBq (2 mCi) [^{18}F]FDG was injected intravenously 4 days after turpentine inoculation and the animals were killed 1 hr later. Inflammatory tissues were dissected immediately and samples were embedded in an O.C.T compound (Miles Inc. Elkhart, IN) and frozen with dry ice. The frozen samples were sectioned in a cryostat at −20 °C. They were processed for macro- and micro-autoradiography as described previously (*21*). Briefly, 10-μm thick sections used in the macro-autoradiography study were mounted on clean glass slides, air-dried and contacted with autoradiography film (MARG ^{3}H-type, Konica, Tokyo, Japan). After exposure for 1 hr, the films were processed photographically. Sections on the slides were stained with hematoxylin and eosin, and examined under a light microscope.

Contiguous 5-μm thick frozen sections used in micro-autoradiography study were directly mounted on slides coated with NTB2 nuclear emulsion (Eastman Kodak, Rochester, NY) under a safety light. Slides were immediately deep-frozen on dry ice and placed in an exposure box cooled with dry ice. After exposure for 6 hr, slides were histologically fixed and processed photographically. Sections of micro-autoradiography were stained with hematoxylin and eosin. The number of silver grains in the micro-autoradiography was counted in various regions of the inflammatory tissue under a light microscope using a micrometer.

Part of the inflammatory tissue was fixed in 10% formalin and embedded in paraffin. Thin sections were stained with hematoxylin and eosin for histological examination.

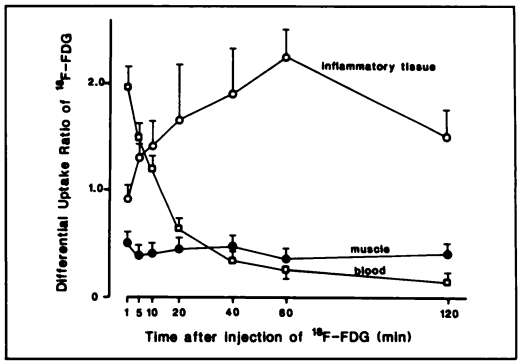

FIGURE 1. Time-course of [^{18}F]FDG uptake in inflammatory tissue, muscle and blood. Rats were injected with [^{18}F]FDG 4 days after inoculation with turpentine oil (n = 5, each time after injection).

RESULTS

Time-Course Study of Fluorine-18-FDG Tissue Distribution

Figure 1 illustrates [^{18}F]FDG uptake at various time intervals after injection. The uptake of [^{18}F]FDG in inflammatory tissue gradually increased until 60 min and then decreased. Therefore, the remainder of experiments were performed 60 min after injection of [^{18}F]FDG. The blood level was highest at 1 min but rapidly decreased thereafter. The uptake in muscle was low and almost constant.

Longitudinal Study of Fluorine-18-FDG Tissue Distribution

Figure 2 demonstrates the uptake of [^{18}F]FDG measured on several days after inoculation of turpentine oil. The uptake of [^{18}F]FDG by inflammatory tissue progressively increased to a peak level 4 days after inoculation, and then decreased. The maximum DUR observed on Day 4 was 1.5 and approximately 3.2 times that measured on the same day in muscles. The uptake in muscle and blood level were small and did not change throughout the 2-wk period of observation.

A typical turpentine-induced inflammatory tissue is shown in Figure 3. One day after inoculation (Fig. 3A),

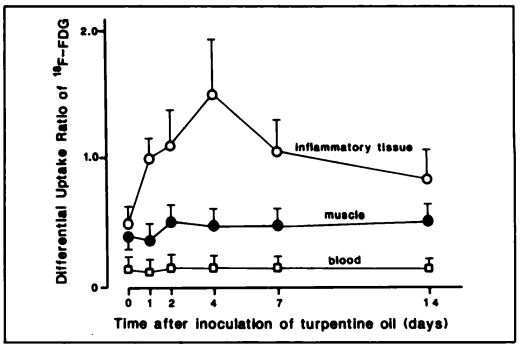

FIGURE 2. Fluorine-18-FDG uptake in inflammatory tissue, muscle and blood several days after inoculation with turpentine oil. A control group without the inoculation was designated as Day 0 (n = 5, each day after inoculation).

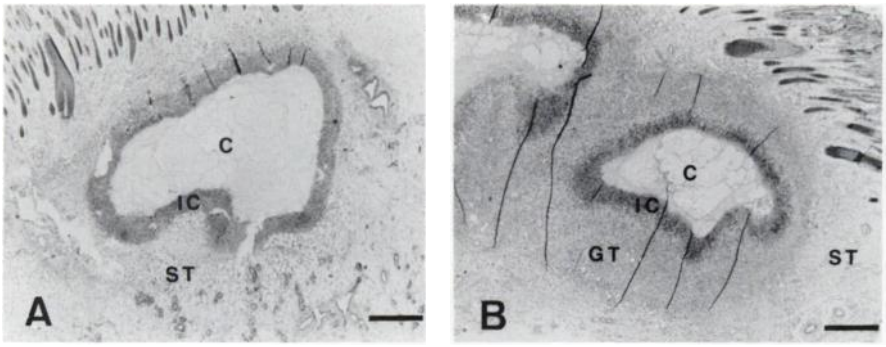

FIGURE 3. Photomicrographs of formalin-fixed sections of turpentine-induced inflammatory tissue stained by hematoxylin and eosin. (A) Center of inflammatory tissue (C) surrounded by inflammatory cells (IC) and edematous subcutaneous tissue (ST) 1 day after inoculation with turpentine oil. (B) The center (C) surrounded by inflammatory cells (IC), thick granulation tissue (GT) and edematous subcutaneous tissue (ST) 4 days after inoculation. Scale bar: 0.4 mm. Note the presence of granulation tissue in (B) but not in (A).

turpentine oil was observed in the center of the inflammatory tissue, surrounded by inflammatory cells and edematous subcutaneous tissue. Four days after inoculation (Fig. 3B) when maximum [^{18}F]FDG uptake was observed, the center of the inflammatory tissue, consisting of turpentine oil and cell debris, was surrounded by a thin inflammatory cell layer and a thick granulation tissue. There was a notable histological difference between Days 1 and 4 regarding the absence (Fig. 3A) or presence of granulation tissue (Fig. 3B).

Macro-Autoradiography and Micro-Autoradiography

A typical [^{18}F]FDG macro-autoradiogram with the corresponding section of inflammatory tissue 4 days after inoculation of turpentine oil is shown in Figure 4. Fluorine-18-FDG macro-autoradiography (Fig. 4A) demonstrated a high density of silver grains in the surrounding zone that corresponded histologically to the abscess wall of the inflammatory cell layer and granulation tissue (Fig. 4B). The density was very low in the center of the inflammatory tissue and low in the subcutaneous tissue.

Figure 5 is a photomicrograph of the formalin-fixed section of inflammatory tissue 4 days after inoculation of turpentine oil. The inflammatory tissue was divided into five distinct histological areas: an abscess center, a neutrophil layer, a marginal zone, granulation tissue and subcutaneous tissue. The abscess center consisted of turpentine oil and cell debris. In the neutrophil layer, a large number of round and polymorphonuclear cells were observed near the adjacent peripheral marginal zone, with dead cells and exudate observed near the center. In the marginal zone, endothelial cells of blood vessels, young fibroblasts and round cells of phagocytes of macrophage and neutrophil were present. Flat cells of matured fibroblast and a few macrophages were observed in the granulation tissue. The neutrophil layer, marginal zone and granulation tissue formed the wall of the abscess. In the subcutaneous tissue, fibroblasts and round cells were seen, but the distance between cells was greater than that in normal subcutaneous tissue, indicating edematous tissue.

Figure 6 shows typical [^{18}F]FDG micro-autoradiograms of the abscess wall 4 days after inoculation of turpentine oil. The highest grain density was found in the marginal zone.

A good linear relationship exists between grain numbers and the corresponding [^{18}F]FDG radioactivity of the section in micro-autoradiography within the range of grain number of 0–50 grains/100 μm^2 (*21*). In the present study, micro-autoradiography was performed within the confirmed range of linearity.

Table 1 summarizes the results of grain counting on [^{18}F]-FDG micro-autoradiography of abscess wall 4 days after inoculation of turpentine oil. The lowest grain density was found in the center of the abscess, while the highest was present in the marginal zone (12.1 times that of the center), followed by the neutrophil layer (5.7 times) and granulation tissue (4.1 times). Cell density was measured in the formalin-fixed section of Figure 5 and listed in Table 1. A weak-positive correlation ($r = 0.883$) between cell density and the degree of [^{18}F]FDG uptake was observed, but was not statistically significant (Student's t-test; $p = 0.11$).

DISCUSSION

Inflammation has been referred to historically as either acute or chronic, depending on the persistence of injury and the nature of inflammatory response (*22,23*). Acute inflammation is characterized by increased vascular permeability with exudation of plasma and migration of neutrophils. On the other hand, chronic inflammation is char-

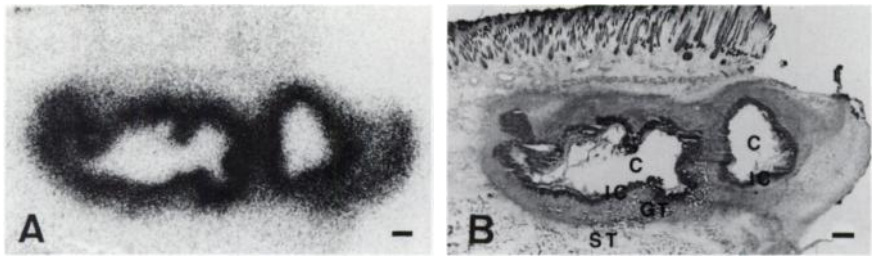

FIGURE 4. Macro-autoradiogram (A) and the corresponding section (B) of inflammatory tissue 4 days after inoculation with turpentine oil. Abbreviations as in Figure 3. Scale bar: 0.4 mm.

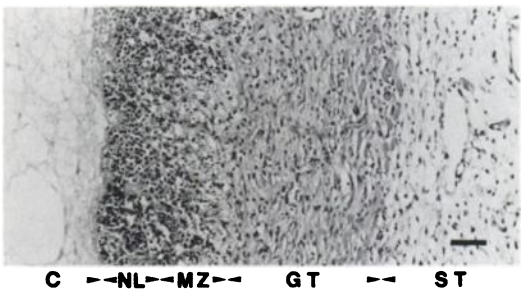

FIGURE 5. A photomicrograph of formalin-fixed section of abscess wall 4 days after inoculation with turpentine oil. Abbreviations as in Figure 3. NL = neutrophil layer. MZ = marginal zone. Scale bar: 50 μm.

acterized by fibroblast proliferation and neovascularization with mononuclear cell infiltration (macrophages, lymphocytes and plasma cells). If the area of acute inflammation is walled off by the collection of inflammatory cells, destruction of the tissue by neutrophil products leads to the formation of an abscess (*23*). Since abscess formation is caused by bacteria or fungi in humans (*9–12*), we tried to use a bacterial inflammation model by inoculating Escherichia coli (*E. coli*) rather than turpentine oil. However, our attempts failed to produce a stable model due to poor bacteriological techniques. Based on the fact that not all bacterial infection led to abscess formation (*24*), we used a turpentine oil-induced inflammatory tissue model since it is easily prepared and is a stable model showing an abscess formation. The characteristics of acute inflammation occurred on the first day after inoculation, while those typical of chronic inflammation were observed at a later stage. Thus, a nonbacterial inflammation model was used in the present study to histologically examine the [^{18}F]FDG uptake and distribution in inflammatory tissue.

Serial PET images of croton oil-induced inflammatory tissue in the rabbit following injection of [^{18}F]FDG during a 60-min period showed that tracer uptake increased slightly during the first 20 min after injection, but was relatively constant thereafter (*25*). In contrast, our time-course study of [^{18}F]FDG tissue distribution demonstrated that [^{18}F]FDG uptake in turpentine-induced inflammatory tissue increased until 60 min postinjection and then decreased. The difference between two studies may be due to differences in the nature of the inflammatory tissue, or may reflect the different methods used in both experiments (PET versus tissue distribution study).

Several investigators reported that the maximum uptake of glucose (^{14}C-glucose and ^{3}H-deoxyglucose) in different wound models were observed at 2–5 days after injury (*14–16*). Our longitudinal study of [^{18}F]FDG tissue distribution in turpentine-induced inflammatory tissue showed that the maximum uptake was observed on Day 4 postinjury. A common finding in these studies was that the maximum uptake did not occur immediately after injury, but rather, several days later. The histological examination of inflammatory tissue in the present study showed the characteristic features of acute inflammation, including migration of neutrophils and edematous subcutaneous tissue on the first day after injury, and that of chronic inflammation with fibroblasts and vascular proliferation and macrophage infiltration on Day 4. These results suggest that glucose utilization in inflammatory tissue is more active during the process of chronic inflammation than that of acute inflammation. In this regard, the use of [^{18}F]FDG may not produce clear images of turpentine-induced inflammatory tissue, as reported by Som et al. (*8*), However, this result may be due to a lack of [^{18}F]FDG uptake in acute inflammation. Clinical PET studies representing high [^{18}F]FDG uptake by human abscesses were performed 10 days to several months after the onset of inflammation (*9–12*). It is obvious that these cases were considered chronic, as they were characterized by chronic inflammation.

In the time-course and longitudinal studies of [^{18}F]FDG tissue distribution, the DURs in the inflammatory tissue at 60 min after [^{18}F]FDG injection and 4 days after inoculation were significantly different (2.3 ± 0.2, 1.5 ± 0.4, respectively, $p < 0.01$). Since each study was performed on a different day, various factors may have affected the value

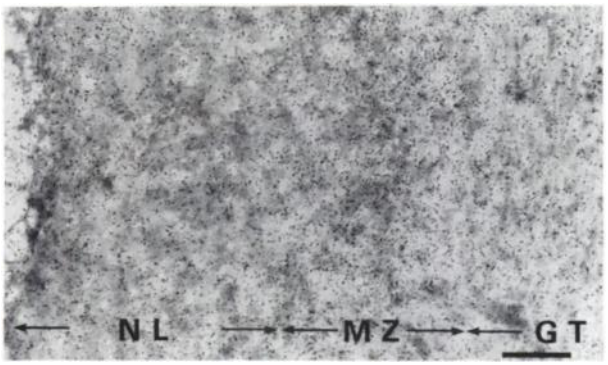

FIGURE 6. Micro-autoradiogram of abscess wall 4 days after inoculation with turpentine oil corresponding to Figure 5. Scale bar: 40 μm.

TABLE 1
Grain Counting on Fluorine-18-FDG Micro-Autoradiography of Inflammatory Tissue Four Days after Inoculation with Turpentine Oil

Area	Grain count	Ratio-to-center	Cell count*
Center	2.8 ± 1.0	1.0	—
Neutrophil layer	16.0 ± 1.8	5.7	14.6 ± 1.7
Marginal zone	33.9 ± 4.0	12.1	17.3 ± 2.8
Granulation tissue	11.4 ± 2.8	4.1	5.4 ± 0.9
Edematous subcutaneous tissue	5.4 ± 1.0	1.9	2.3 ± 0.8

*Cell density was measured in the formalin-fixed section of Figure 5.
Grain count (in grains/100 μm^2) and cell count (number/1000 μm^2) represent the mean ± s.d. of 8–10 measured points within the same lesion.

of DUR, including the biological state of the rat (blood sugar, body weight, movement, etc.), the size of inflammatory tissue and technical errors associated with minute differences in the volume of injected [^{18}F]FDG and standard [^{18}F]FDG used for DUR calculation.

Macro-autoradiography of wounded skeletal muscle shows localization of ^{3}H-DG in the cellular infiltrate within the wound (*26*). This is in agreement with our macro- and micro-autoradiographic studies of [^{18}F]FDG. Our macro-autoradiography study of inflammatory tissue 4 days after inoculation of turpentine oil demonstrated a high [^{18}F]FDG uptake in the abscess wall and surrounding granulation tissue. In addition, micro-autoradiography showed that the highest silver grain density was found in the marginal zone of the abscess wall (followed by the neutrophil layer) and a weak positive correlation between cell density and the degree of the [^{18}F]FDG uptake. It is possible that increased blood flow in the inflammatory tissue, together with increased permeability of capillary blood vessels, results in a leakage of fluid into the extravascular space. Several young fibroblasts and phagocytes (macrophages and neutrophils) were observed in the marginal zone and a large number of neutrophils were present in the neutrophil layer. This suggests that macrophages and neutrophils in inflammatory tissue utilize glucose as an energy source for chemotaxis and phagocytosis (*16,27–29*), while fibroblasts utilize the same substance for proliferation (*30–32*). Our previous micro-autoradiography study in tumor tissue showed that accumulation of [^{18}F]FDG was relatively higher in macrophages and younger granulation tissue than in tumor cells (*21*). Similarly, a high accumulation of [^{18}F]FDG in macrophages and granulation tissue was observed in the present study. However, our results indicate that it is difficult to differentiate between tumor tissue and inflammatory tissue using high [^{18}F]FDG uptake. Results of the present micro-autoradiography study suggest that endothelial cells of blood vessels also utilize glucose for proliferation, but few studies have been reported on this subject.

It is well known that abscess-forming bacteria utilize glucose as an energy source (*33–35*). The results of our preliminary experiments using [^{18}F]FDG macro- and micro-autoradiography of *E. coli* abscesses were similar to those obtained from turpentine inoculation. However, it was not clear whether or not [^{18}F]FDG accumulated in *E. coli*. Further investigation is needed.

CONCLUSION

Our tissue distribution study demonstrated that [^{18}F]FDG accumulated in experimental inflammatory tissue and the maximum uptake was observed in the chronic phase characterized histologically by chronic inflammation. Macro-autoradiography showed that high density of silver grain due to [^{18}F]FDG distribution was found in the abscess wall of inflammatory cell layer and granulation tissue. Micro-autoradiography showed that the highest grain density was found in the marginal zone containing young fibroblasts, endothelial cells of blood vessels, and phagocytes of macrophages and neutrophils. These results will help us understand the high uptake of [^{18}F]FDG in abscesses in humans. We believe that [^{18}F]FDG PET may be a useful tool to detect and monitor chronic inflammatory process.

ACKNOWLEDGMENTS

The authors thank the staff of the Cyclotron and Radioisotope Center, Tohoku University, for their cooperation, Mr. Y. Sugawara for photography and Dr. F. G. Issa (Word-Medex) for his assistance in reading and editing the manuscript. This work was supported by grants-in-aid (06670899, 07274205, 06454320 and 04557047) from the Ministry of Education, Science and Culture, Japan.

REFERENCES

1. Phelps ME, Hunang SC, Hoffman EJ, et al. Tomographic measurement of local cerebral glucose metabolic rate in humans with (F-18)-2-fluoro-2-deoxy-D-glucose: validation of method. *Ann Neurol* 1979;6:371–388.
2. Hawkins RA, Phelps ME, Hunang SC. Effects of temporal sampling, glucose metabolic rates and disruptions of the blood-brain barrier on the FDG model with and without a vascular compartment: studies in human brain tumors with PET. *J Cereb Blood Flow Metab* 1986;6:170–183.
3. DiChiro G, DeLaPaz RL, Brooks RA, et al. Glucose utilization of cerebral gliomas measured by [^{18}F]fluorodeoxyglucose and positron emission tomography. *Neurology* 1982;32:1323–1329.
4. Marshall RC, Tillisch JH, Phelps ME, et al. Identification and differentiation of resting myocardial ischemia and infarction in man with positron computed tomography, ^{18}F-labeled fluorodeoxyglucose and N-13 ammonia. *Circulation* 1983;67:766–788.
5. Tillisch J, Brunken R, Marshall R, et al. Reversibility of cardiac wall-motion abnormalities predicted by positron emission tomography. *N Engl J Med* 1986;314:884–888.
6. Kubota K, Matsuzawa T, Fujiwara T, et al. Differential diagnosis of lung tumor with positron emission tomography: a prospective study. *J Nucl Med* 1990;31:1927–1932.
7. Yonekura Y, Benua RS, Brill AB, et al. Increased accumulation of 2-deoxy-2-^{18}F-fluoro-D-glucose in liver metastasis from colon carcinoma. *J Nucl Med* 1982;23:1133–1137.
8. Som P, Atkins HL, Bandoypadhyay D, et al. A fluorinated glucose analog, 2-fluoro-2-deoxy-D-glucose (F-18): nontoxic tracer for tumor detection. *J Nucl Med* 1980;21:670–675.
9. Tahara T, Ichiya Y, Kuwabara Y, et al. High [^{18}F]fluorodeoxyglucose uptake in abdominal abscess: a PET study. *J Comput Assist Tomogr* 1989; 13:829–831.
10. Sasaki M, Ichiya Y, Kuwabara Y, et al. Ringlike uptake of [^{18}F]FDG in brain abscess: a PET study. *J Comput Assist Tomogr* 1990;14:486–487.
11. Hanson MW, Glantz MJ, Hoffman JM, et al. FDG-PET in the selection of brain lesions for biopsy. *J Comput Assist Tomogr* 1991;15:796–801.
12. Meyer MA, Frey KA, Schwaiger M. Discordance between F-18 fluorodeoxyglucose uptake and contrast enhancement in a brain abscess. *Clin Nucl Med* 1993;18:682–684.
13. Wilmore DW, Aulick LH, Mason AD, et al. Influence of the burn wound on local and systemic responses to injury. *Ann Surg* 1977;186:444–458.
14. Nelson KM, Turinsky J. Local effect of burn on skeletal muscle insulin responsiveness. *J Surg Res* 1982;31:288–297.
15. Tischler ME, Fagan JM. Response to trauma of protein, amino-acid, and carbohydrate metabolism in injured and uninjured rat skeletal muscles. *Metabolism* 1983;32:853–868.
16. Daley JM, Shearer JD, Mastrofrancesco B, et al. Glucose metabolism in injured tissue: a longitudinal study. *Surgery* 1990;107:187–192.
17. Lear JL, Ackerman R, Kameyama M, et al. Multiple-radionuclide autoradiography in evaluation of cerebral function. *J Cereb Blood Flow Metab* 1984;4:264–269.
18. Fuglsang A, Lomholt M, Gjedde A, et al. Blood-brain transfer of glucose and glucose analogs in newborn rats. *J Neurochem* 1986;46:1417–1428.
19. Redies C, Matsuda H, Diksic M, et al. In vivo measurement of [^{18}F]fluorodeoxyglucose rate constants in rat brain by external coincidence counting. *Neurosci* 1987;22:593–599.

20. Kubota K, Ishiwata K, Kubota R, et al. Tracer feasibility for monitoring tumor radiotherapy: a quadruple tracer study with fluorine-18-fluorodeoxyglucose or fluorine-18-fluorodeoxyuridine, l-[methyl-^{14}C]methionine, [6-^{3}H]thymidine, and gallium-67. *J Nucl Med* 1989;30:2012–2016.
21. Kubota R, Yamada S, Kubota R, et al. Intratumoral distribution of fluorine-18-fluorodeoxyglucose in vivo: high accumulation in macrophages and granulation tissues studied by microautoradiography. *J Nucl Med* 1992;33:1972–1980.
22. Wilhelm DL. Inflammation and healing. In: Anderson WAD, Kissane JM, eds. *Pathology*, seventh edition. St Louis: C.V. Mosby Co.; 1977:25–89.
23. Fantone JC, Ward PA. Inflammation. In: Rubin E, Farber JL, eds. *Pathology*, second edition. Philadelphia: J.B. Lippincott Co.; 1994:33–66.
24. Brook I, Walker RI. Infectivity of organisms recovered from polymicrobial abscesses. *Infect Immun* 1983;42:986–989.
25. Fukuda H, Yoshioka S, Watanuki S, et al. Experimental study for cancer diagnosis with ^{18}FDG: differential diagnosis of inflammation from malignant tumor. *Jpn J Nucl Med* 1983;20:1189–1192.
26. Forster J, Morris AS, Shearer JD, et al. Glucose uptake and flux through phosphofructokinase in wounded rat skeletal muscle. *Am J Physiol* 1989; 256:788–797.
27. Weisdorf DJ, Craddock PR, Jacob HS. Glycogenolysis versus glucose transport in human granulocytes: differential activation in phagocytosis and chemotaxis. *Blood* 1982;60:888–893.
28. Shearer JD, Amaral JF, Caldwell MD. Glucose metabolism of injured skeletal muscle: the contribution of inflammatory cells. *Circ Shock* 1988;25:131–138.
29. Cline MJ, Lehrer RI. Phagocytosis by human monocytes. *Blood* 1968;32: 423–435.
30. McKey ND, Robinson B, Brodie R, et al. Glucose transport and metabolism in cultured human skin fibroblasts. *Biochem Biophys Acta* 1983;762: 198–204.
31. Kittlick PD. Fibrin in fibroblast cultures—a metabolic study as a contribution to inflammation and tissue repair. *Exp Path* 1979;17:312–326.
32. Landes BD, Lemonnier F, Couturier M, et al. Comparative metabolic effects of fructose and glucose in human fibroblast cultures. *In Vitro Cell Dev Biol* 1987;23:355–360.
33. Senez JC. Some considerations on the energetics of bacterial growth. *Bacteriol Rev* 1962;26:95–107.
34. Gibbs M, DeMoss RD. Anaerobic dissimilation of C14-labelled glucose and fructose by pseudomonas lindneri. *J Biol Chem* 1954;207:689–694.
35. Forrest WW. Energies of activation and uncoupled growth in streptococcus faecalis and zymomonas mobilis. *J Bacterio* 1967;94:1459–1463.